Marine Pollution Bulletin 162 (2021) 111887

Contents lists available at ScienceDirect

Marine Pollution Bulletin

journal homepage: www.elsevier.com/locate/marpolbul

Microplastics on the sea surface of the semi-closed Tokyo Bay

Haruka Nakano *, Hisayuki Arakawa, Tadashi Tokai

Tokyo University of Marine Science and Technology, Konan 4-5-7, Minato-ku, Tokyo 108-8477, Japan

ARTICLE INFO

Keywords:
Microplastics
Semi-closed bay
Seasonal variation
Tokyo Bay

ABSTRACT

Microplastics (MPs) pollution surveys were conducted in Tokyo Bay using neuston nets (May 2019 and January 2020). Although the pollution level in Tokyo Bay was high (3.98 pcs/m^3, May), it was lower than reported in other semi-closed bays because of differences in the Enclosed Index. It was found that polyethylene fragments dominated the retrieved MPs; the mode of MPs size was 800 μm. As MPs abundance in rivers had the same seasonality as found in the inner bay, rivers were considered the main source of MPs. The seawater residence time is shorter than the time required for the density of MPs to become greater than that of seawater; therefore, it was considered that MPs are transported out of the bay instead of sinking. MPs were aggregated into a convergence zone by residual currents (the thermohaline front) in May (January). These findings will improve understanding of MPs pollution in other bays.

1. Introduction

Huge amounts of waste plastics are transported into the oceans via various routes due to human activities and accidents (e.g., Andrady, 2011). Of the total amount of waste plastics transported into the oceans, only 1% is found as marine debris; the remaining 99% is lost and termed "missing plastics" (e.g., Cózar et al., 2014). Therefore, many surveys have been conducted to determine the fate of this type of marine debris (e.g., Isobe et al., 2015). Generally, two candidate fates are considered. The first involves the breaking of particles of debris into small pieces called microplastics (MPs: longest diameter < 5 mm), and the other involves particles sinking to the seafloor (e.g., Matsuguma et al., 2017). However, as conclusive information remains lacking, further investigation of plastic pollution is required, especially as the effect of MPs on ecosystems globally is an important concern (e.g., Andrady, 2011).

Previous research on MPs has shown that waters near regions with high urban ratios and inadequate waste treatment systems are highly polluted (e.g., Kataoka et al., 2019). This indicates that river water with high concentrations of MPs flow into coastal areas. If transportation of MPs into coastal waters via rivers were a continuous process (e.g., Horton and Dixon, 2018), then it should be expected that the abundance of MPs in coastal waters would increase if there were no route for removal. In particular, semi-closed and enclosed bays that retain chemical substances input via rivers represent strong candidates for the storage of MPs; however, the residence time and behavior of MPs in such water bodies have not been investigated previously. In addition, in estuary regions, the physical conditions of ocean waters (e.g., residual currents and fronts) should be considered because such conditions can generate convergence zones in which particles of marine debris could gather (e.g., Miyao and Isobe, 2016; Zheng et al., 2019).

Accordingly, this study focused on Tokyo Bay, which is a semi-closed bay in the center of Japan (Fig. 1a). Previous studies reported that MPs represent one of the most serious marine pollutants in this bay. For example, 77% of Japanese anchovy (*Engraulis japonicus*) caught in the bay were found to have ingested MPs (Tanaka and Takada, 2016). Moreover, microbeads were found to account for 6% of the total MPs pollution load (Isobe, 2016).

Although MPs pollution in Tokyo Bay is evident, comprehensive understanding of the problem remains lacking. One of the reasons is that full details of MPs pollution in Tokyo Bay have not been elucidated. Another reason is inadequate evaluation of the role of rivers as a source of MPs pollution. Based on previous related research on both the seasonality in the abundance of MPs and the urban ratio (e.g., Cheung et al., 2016; Eo et al., 2019; Kataoka et al., 2019), the metropolitan area in the wet season could be considered a potential source of the MPs found in Tokyo Bay. In Japan, precipitation in summer is greater than in other seasons.

Consequently, focusing on MPs pollution in Tokyo Bay, the objectives of this study were as follows: (1) to compare the abundance of MPs with that in other regions, (2) to report comprehensive information relating to MPs, (3) to evaluate the role of rivers as a source of MPs, (4) to investigate the fate of MPs, and (5) to reveal the pattern of

* Corresponding author.
E-mail addresses: hnakan2@kaiyodai.ac.jp (H. Nakano), arakawa@kaiyodai.ac.jp (H. Arakawa), tokai@kaiyodai.ac.jp (T. Tokai).

https://doi.org/10.1016/j.marpolbul.2020.111887
Received 1 October 2020; Received in revised form 25 November 2020; Accepted 26 November 2020
Available online 8 December 2020

distribution of MPs in Tokyo Bay.

2. Data and methods

2.1. Field survey of MPs

Tokyo Bay, located in the center of Japan and surrounded by the Tokyo metropolitan area, faces the North Pacific Ocean (Fig. 1a). Four main rivers discharge into the western side of the bay (i.e., the Edogawa River, Arakawa River, Tamagawa River, and Tsurumigawa River; Fig. 1b). The total area of the basins of these four rivers is approximately 4.7×10^9 m^2, supporting a population of 16 million people.

Sampling campaigns in this bay were conducted in May 2019 using training vessel (T/*V*) *Seiyo-Maru*, and in January 2020 using both research vessel (R/V) *Hiyodori* and T/V *Seiyo-Maru*. Observation points were deployed at inner (three points: Stns. 51, S02, S03) and outer (two points: Stns. S08, 00) parts of the bay (Fig. 1). Field sampling was conducted using a neuston net (5552; RIGO Co., Ltd., Tokyo, Japan) with net mouth, net length, and mesh size of 0.75 × 0.75 m, 3 m, and 350 μm, respectively. The net was towed for durations of 10–20 min at a speed of 2 knots (Table S1). The amount of floating debris collected in the net was attributed to the actual duration. A flowmeter (5571A; RIGO Co., Ltd.) was installed at the net mouth to measure the water volume passing through during sampling (e.g., Isobe, 2016). Samples of seawater containing MPs were placed in polyvinyl chloride bottles, which were stored in the dark prior to undergoing the preprocessing process.

2.2. Preprocessing process

Before commencing the analysis procedure, all equipment was washed using distilled water. After filtration of the seawater sample through a sieve (mesh size: 100 μm) made of polyamide with a polyvinyl chloride frame, the filtered samples were collected in a beaker. As the mesh size of the sieve was 100 μm, fragments of MPs whose shortest length was <140 μm might have been lost (e.g., Michida et al., 2019), which means the abundance of smaller particles might have been underestimated. However, the mesh size of the sieve (100 μm) was smaller than the mesh size of the neuston net (350 μm); therefore, it was considered that most particles were collected. To remove organic matter, 25–60 ml 30% H_2O_2 (the actual amount depended on the sample volume) and 25 ml 0.05 M Fe (2) solution were added (e.g., Masura et al., 2015). If any natural organic matter remained, an additional amount of 30% H_2O_2 was added to the samples, repeatedly. To eliminate contaminants, these samples were heated on a hot magnetic stirring plate with a maximum speed of 100 rpm. As we followed the protocol of Masura et al. (2015), we set the temperature to 60–75 °C in May. However, as the size might be affected by high temperatuers (>70 °C; e.g., Munno et al., 2018), we used the mild temperature of 40–60 °C in January (Gago et al., 2018). In the early stage of heating, the lower temperature was used to avoid bumping. As the amount of organic matter was greater in May than in January, this procedure was conducted over a 14-d (6-d) period for the summer (winter) samples.

2.3. Density separation

After eliminating the H_2O_2 solution using a sieve with mesh size of 100 μm, the samples were collected in a beaker and NaI solution with density of 1.5 g/cm^3 was added. The sample was mixed, left to stand for at least 1 h, and then individual particles were collected. The mixing and picking processes were performed three times for each sample. The remaining medium was checked under a stereomicroscope ("nano.capture" Sightron Japan, Inc.).

2.4. Measurement and identification

The maximum length of particles (hereafter, size) was measured using "ImageJ" software and photos taken by a digital stereomicroscope ("nano.capture" Sightron Japan, Inc.). As Andrady (2011) divided MPs into two groups (i.e., primary and secondary), we classified the MPs

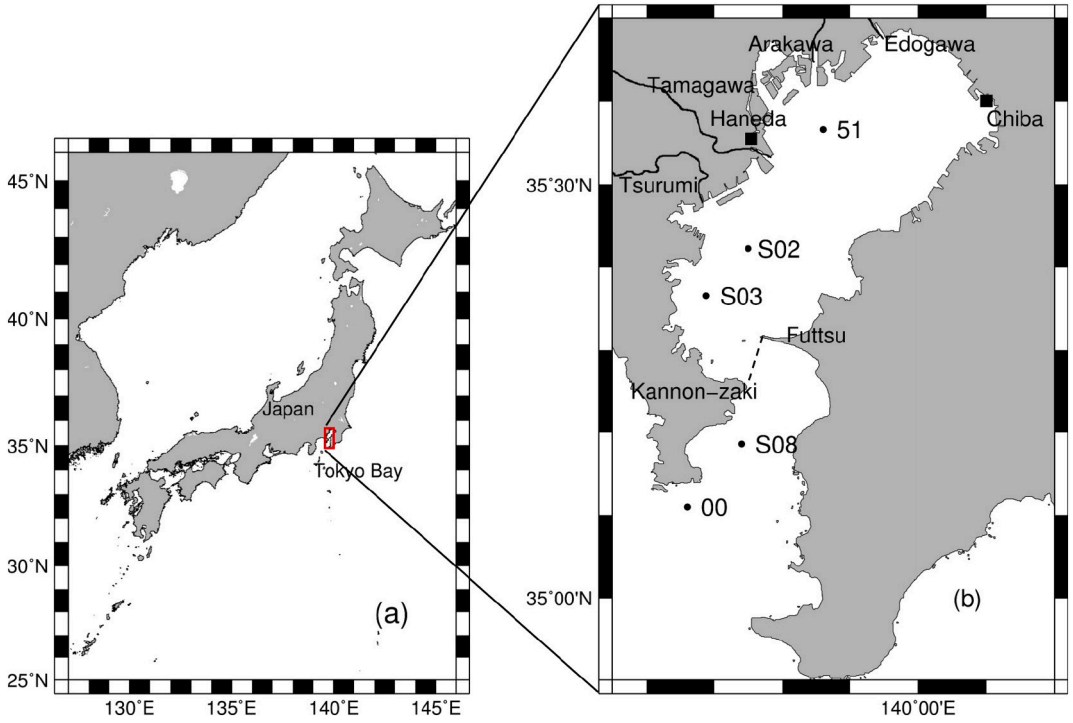

Fig. 1. Study area: (a) location of Tokyo Bay and (b) enlarged view of area shown by the rectangle outlined in panel (a). Symbols and lines in panel (b) show neuston net sampling stations (black dots), meteorological observation stations at Haneda and Chiba (black squares), and main rivers discharging into Tokyo Bay (black lines, Edogawa River, Arakawa River, Tamagawa River, and Tsurumigawa River). Dashed line represents the border between the inner bay and the outer bay.

found in this study into two such categories. Primary MPs are small particles used directly (e.g., microbeads that are included in cosmetics and toothpaste, and resin pellets that constitute the raw component of plastic products), whereas secondary MPs are pieces of large plastic items broken through weathering processes. The characteristics of the MPs were recorded based on the categories advocated by GESAMP (2019) with six shapes (i.e., primary MPs: microbeads and resin pellets; secondary MPs: fragment, foam, film, and line) and 13 colors (i.e., nonpigmented: clear and opaque, and pigmented: white, black, brown, blue, green, orange, red, pink, purple, and yellow).

Infrared spectra of candidate particles were measured using the attenuated total reflection method of Fourier transfer infrared spectroscopy (IR/FT-6600, JASCO Inc., Japan; hereafter, FTIR). The background spectra comprised ensemble averages of 32 members. The sample spectra comprised ensemble averages of 16 members with resolution of 4 cm^{-1} and a wavenumber range of 400–4000 cm^{-1}.

To identify the detailed composition, the measured sample spectra were compared with library data from "KnowItAll" provided by Bio-Rad Laboratories, Inc., USA (e.g., Renner et al., 2018). Precision was verified by the Hit Quality Index (HQI), which represents the degree of agreement between the spectra and the library data. The HQI range is between 0 and 100. If the HQI value was ≥60, we accepted it as a library material; if the HQI value was <60, the candidate was recorded as nonplastic (e.g., Hanke et al., 2013). In this study, we focused on MPs with an HQI value of ≥60. For the calculation of the HQI, we ignored the effects of both CO_2 (650–700 cm^{-1} and 2250–2450 cm^{-1}) and strong instrumental noise (<500 and >4000 cm^{-1}).

2.5. Abundance per area

Abundance per area N_{Area} (pcs/m^2) was calculated using the following equation (Kukulka et al., 2012):

$$N_{Area} = N_0 A_0 / w, \quad (1)$$

where N_0 (pcs/m^3) is the abundance per volume of MPs in the sample obtained by the neuston net, A_0 (m^2/s) is a parameter related to significant waves and wind, and w is the rise velocity of MPs (5.3×10^{-3} m/s, Reisser et al., 2015). In this study, A_0 was calculated using the following equation:

$$A_0 = 1.5 u^* \kappa H_s, \quad (2)$$

where u^* (m/s) is the frictional velocity of water, estimated as $0.0012 \times W_{10}$ (m/s, W_{10} is the wind velocity at the height of 10 m); κ is the von Karman coefficient, set to 0.4; and H_s (m) represents the significant wave height. Both W_{10} and H_s were provided by the Bureau of Ports and Harbors of the Tokyo metropolitan government (https://www.kouwan.metro.tokyo.lg.jp/yakuwari/choui/kako1-index.html).

2.6. MPs abundance from rivers

The flow rate of a river V (m^3/s) can be estimated based on summation of the upstream flow rate Vu (m^3/s) and downstream flow rate Vd (m^3/s), which can be calculated using the basin area S (m^2), precipitation P (m/s), and an outflow constant (=0.6) as follows (e.g., Matsumura and Ishimaru, 2004):

$$V = V\mathrm{u} + V\mathrm{d} = V\mathrm{u} + 0.6SP. \quad (3)$$

To estimate the flow rates of the rivers in May and January, we used flow rate data and precipitation data from 2018, which were measured at several observation sites around Tokyo Bay, i.e., Nagareyama and Shinozaki for the Edogawa River, Ishihara and Denenchohu for the Tamagawa River, and Kamenokobashi and Kawasaki for the Tsurumigawa River (summarized in Table S2). For the Arakawa River, flow rates were obtained from the Japan River Association (2004). Parameters Vu and P were obtained from the water information system of the Ministry of Land, Infrastructure, Transport, and Tourism (http://www1.river.go.jp/).

The abundance of MPs in the rivers was calculated using values of 2.26 and 0.03 pcs/m^3 for May and December, respectively, which were derived from the supplemental data of Kataoka et al. (2019). From the product of the abundance, the flow rates of river discharge, and the inner bay area (9.2×10^8 m^2, 920 km^2), the abundance per unit area of the inner bay was calculated for both May and December (Table S3).

2.7. Geographic characteristics of Tokyo Bay

We considered the geographical characteristics of Tokyo Bay as defined by the Enclosed Index (*E.I.*; e.g., Baba and Imamoto, 1998; Nakao and Matsuzaki, 1995) for standardization and comparison of MPs pollution:

$$E.I. = \mathrm{sqrt}(S) D_1 / W D_2, \quad (4)$$

where S is the area of the bay, W is the width of the bay mouth, D_1 is the maximum depth, and D_2 is the depth at the bay mouth. As *E.I.* has positive correlation with the residence time of seawater in a bay (Nakao and Matsuzaki, 1995), i.e., a greater value of *E.I.* implies that the degree of closure of a bay is high, the value of *E.I.* reflects how long substances might remain within a bay.

2.8. Blank and recovery test

For the blank test, a Petri dish was set in the laboratory during the experimental procedure to check for contamination. This Petri dish was examined under a microscope and any particles detected were checked using FTIR. Other than for a few fibers, we found no candidate MPs in the blank Petri dish. FTIR verified that the observed fibers were rayon fibers from clothes, not fishing gear; hence, we could safely discount laboratory contamination.

We investigated the recovery rate to verify the possibility of loss of MPs during the procedure described in Sections 2.4 and 2.5. Plastic beads with diameter of 300, 600, and 5000 μm were mixed and used in this test (Table 1). Smaller MPs were considered more difficult to collect (e.g., Isobe et al., 2019); therefore, greater numbers of small particles (300 μm) were used in comparison with larger particles. This test was performed three times. Overall, 96.8% of particles were collected from the recovery test. The individual recovery rate was slightly lower (94.0%) for smaller particles (Table S3). The slightly lower rate of recovery of 300-μm particles was considered a reasonable result because the tendency is that the recovery ratios of smaller particles are lower in comparison with larger particles. This result is similar to the findings reported by Isobe et al. (2019). Moreover, as we used FTIR to identify the composition, our data were considered to have quality equivalent to that of the best-practice data reported in Isobe et al. (2019). These results are summarized in Table S4.

3. Results and discussion

3.1. Abundance of MPs

Although we found 3772 candidate particles of MPs in Tokyo Bay, only 2798 pcs were identified as MPs after following the FTIR procedure. We found 2537 pcs (91% of the total MPs) in May and 261 pcs in January (Table 1). The mean abundance of MPs per volume was 3.98 and 0.55 pcs/m^3 in May and January, respectively; the largest abundance in each month was 17.75 pcs/m^3 at Stn. S03 in May and 2.43 pcs/m^3 at S08 in January (Fig. 2). With the exception of Stn. S08, the abundance of MPs in May was larger than in January; the values in May were approximately 6–116 times greater than in January (Table 1). The mean abundance of MPs per area (N_{Area}) was 0.42 and 0.03 pcs/m^2 in May and January, respectively (Table 1); the maximum abundance was

Table 1
Abundance of MPs in Tokyo Bay.

	Station	Filtered water volume (m^3)		Abundance of MPs (pcs) *		Abundance rate per volume of MPs N_0 (pcs/m^3)		Abundance rate per area N_{Area} (pcs/m^2)	
		May	January	May	January	May	January	May	January
Inner bay	51	226.05	107.30	35 (35)	0 (0)	0.15	–	0.06	–
Outer bay	S02	221.07	93.74	114 (113)	4 (4)	0.52	0.04	0.21	0.01
	S03	124.21	69.30	2205 (2062)	11 (11)	17.75	0.16	1.61	0.01
	S08	84.37	95.96	45 (43)	233 (232)	0.53	2.43	0.05	0.14
	00	147.74	114.84	138 (136)	13 (13)	0.90	0.11	0.18	0.01
Total		–	–	2537 (2389)	261 (260)	3.98**	0.55**	0.42**	0.03**

* Number of secondary MPs is given in parentheses.
** Mean values.

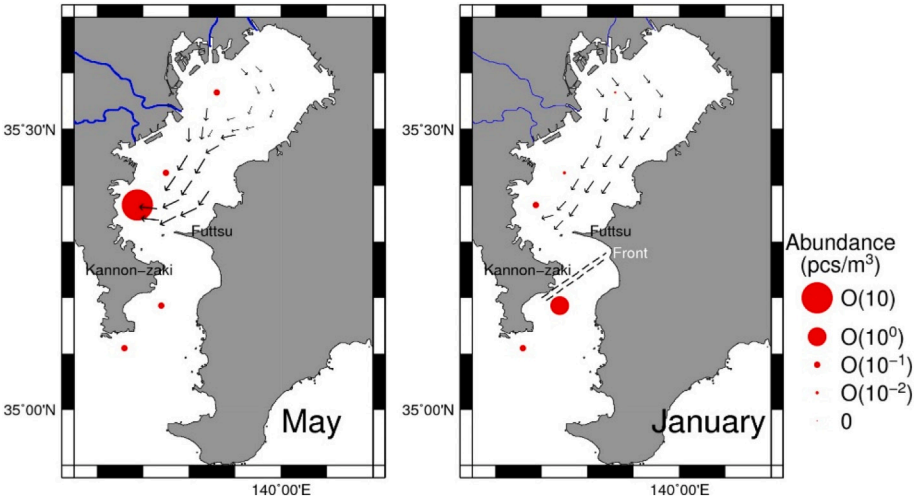

Fig. 2. Abundance of MPs in Tokyo Bay, indicated by the size of red circles (its order was shown as legends), and schematic of residual currents from Suzuki et al. (2012), shown by black arrows, where the thickness of the arrows indicates current strength. (For interpretation of the references to color in this figure legend, the reader is referred to the web version of this article.)

1.61 pcs/m^2 (i.e., 1,610,000 pcs/km^2) at Stn. S03.

In September, one of the months with high precipitation in Japan, spots with high abundance of MPs were observed in the west of Tokyo Bay (Isobe, 2016); the abundance of MPs was 11.1 pcs/m^3 in waters off Haneda and 6.0 pcs/m^3 in waters near the Tsurumigawa River. This study and that of Isobe (2016) found higher abundance of MPs in Tokyo Bay in the wet season than in the dry season (winter in Japan).

The maximum abundance of MPs found in Tokyo Bay in May is comparable with the abundance in the eastern Asian seas as reported by Isobe et al. (2015), i.e., 3.74 pcs/m^3 (1,720,000 pcs/km^2). Moreover, the mean value is larger than that found in several other semi-closed bays, e.g., Hiroshima Bay, Delaware Bay, and Chesapeake Bay (Table 2; Bikker et al., 2020; Chen et al., 2018; Cohen et al., 2019; McEachern et al., 2019; Sagawa et al., 2018; Sutton et al., 2016; Zheng et al., 2019). Therefore, we concluded that Tokyo Bay is one of the areas with the highest level of MPs pollution. However, as the abundance of MPs in Tokyo Bay is lower than that in San Francisco Bay (USA), which has a smaller population than the Tokyo Bay area (7.8 million people), we should consider other standard values for evaluating MPs pollution.

First, we focused on how waste is managed in San Francisco. The waste management system in San Francisco, which is one of the most high-quality systems in the USA, has zero waste as a targeted waste-management manifesto (Zaman and Lehmann, 2013). In San Francisco, the proportions of composted, recycled, and landfilled waste are 20%, 52%, and 28%, respectively, whereas in Japan, 77% of waste is burned, 19% is recycled, and only 1% sent to landfill. Hence, one of the reasons for the abundance of MPs in Tokyo Bay might be the amounts of waste composted and landfilled in the surrounding region.

Next, we focused on the geographic characteristics represented by the value of the *E.I.* Since the *E.I.* value of Tokyo Bay is lower than that of San Francisco Bay (Table 2), it is considered that MPs remain longer in San Francisco Bay than in Tokyo Bay. Additionally, we found a tendency for MPs abundance to be large in a bay that has a high *E.I.* value (Table 2), although there are exceptions that are probably attributable to other local factors (e.g., Chesapeake Bay; Bikker et al., 2020). This implies that a greater quantity of MPs is stored in a bay that has a high degree of closure.

3.2. Characteristics of MPs

(a) Shapes of MPs

All shape types of MPs were found (Fig. S1). Secondary MPs (2649 pcs) accounted for 95% of the total MPs. The fragment shape type occurred most frequently in both May and January (Fig. 3ii and iii), and accounted for 75% of the total secondary MPs; foam contributed 13%, while film and line each accounted for 6% (Fig. 3i). Moreover, the percentage of line differed markedly between May and January, i.e., no

Table 2
Abundance of MPs in several semi-closed bays.

Location	Country		N_0 (pcs/m^3)	N_{area} (pcs/km^2)	Enclosed Index (*E. I.*)
Tokyo Bay	Japan	Present study (upper: May, lower: January)	3.98 ± 6.90 0.55 ± 0.94	422,000 ± 600,000 34,000 ± 53,000	1.78
Hiroshima Bay	Japan	Sagawa et al. (2018)	Not shown	30,000–240,000	1.13*
San Francisco Bay	USA	Sutton et al. (2016)	Not shown	700,000 ± 600,000	7.49
Delaware Bay	USA	Chohen et al. (2019) (upper: April, lower: June)	1.24 ± 0.26 0.62 ± 0.29	1,100,000 ± 220,000 490,000 ± 230,000	3.74
Tampa Bay, Florida	USA	McEachern et al. (2019)	4.5 ± 2.3	Not shown	6.71
Chesapeake Bay	USA	Bikker et al. (2020)	0.16 ± 0.29	Not shown	5.98
Xiangshan Bay	China	Chen et al. (2018)	8.9 ± 4.7	Not shown	15.38
Jiaozhou Bay	China	Zheng et al. (2019)	46 ± 28	Not shown	46.81

* From Seto Inland Sea.

line was found in the January samples (Fig. 3i and iii).

Microbeads comprised 97.32% of the total primary MPs. The largest quantity of microbeads was found at Stn. S03 in May. Four resin pellets (<5 mm) were found at Stns. S03 and 00 in May.

(b) Colors

In the case of fragments, 34% of particles were nonpigmented (clear and opaque) and the remaining particles were pigmented (Fig. 4a-i). The pigmented fragments were mostly white, blue, or green (Fig. 4a-i, ii, and iii). Most pieces of foam were white (86%; Fig. 4b-i), although foam with a black surface was found in January (Fig. 4b-iii), which could be attributed to soiling by oil. Pieces of film were mostly nonpigmented (78%; Fig. 4c-i); pigmented film was found only in May (78%; Fig. 4c-ii and iii). In the case of line, 68% of pieces were pigmented with the color of white, blue, or green (Fig. 4d-i, ii, and iii).

(c) Composition of secondary MPs

We focused on secondary MPs as they constituted 95% of the total. The composition of MPs is shown in Fig. 5. The main composition was polyethylene (PE), followed by copolymers of polypropylene (PP) and PE (Fig. 5a, PE/PP and PP/PE; the former represents the main composition of the copolymer). Furthermore, PE and Acryl copolymers (PE/Acryl) and PE and polyvinyl acetate (PVAc) could not be ignored because they accounted for 5% of the total, which is a contribution similar to that of PP. Except for foam, the composition was almost the same (Fig. 5b, d, and e). In the case of foam, although the main contributor was PP/PE, we could not ignore the contributions of copolymers of PE/PS/Acryl (PS: polystyrene).

(d) Size distribution

The mode of the particle size distribution of all secondary MPs was approximately 800 μm (Fig. 6a), and the occurrence frequency decreased rapidly in the range below 800 μm. Michida et al. (2019) reported that MPs whose longest dimension was equivalent to the mesh size $\times\sqrt{2}$ could pass through a sampling net. In our study, this limitation in relation to our observation net was approximately 500 μm. Additionally, if a neuston net were distorted during the observation, MPs whose longest dimension was 700 μm could pass through the net. Thus, the mode of the size of the MPs collected in this study reflects the mesh-size limitation of the neuston net. Therefore, we intend to focus attention on small-sized MPs in Tokyo Bay in the near future.

Individually, the mode of the size distribution of the fragment type was approximately 800 μm with a tail to the right (Fig. 6b); however, the modes of the other types of secondary MPs were clearly larger (Fig. 6b–e). The Steel–Dwass test showed that significant differences existed in the medians of the size of the MPs categorized by shape type (Fig. 7). In contrast, the size of most primary MPs was <1000 μm.

Additionally, we compared the sizes of fragments categorized by color. The average size ± standard deviation of nonpigmented fragments (1241 ± 825 μm) was clearly smaller than that of pigmented fragments (2030 ± 1083 μm; the size difference was verified by median test, $p < 0.01$), indicating that smaller particles were decolorized more easily when degrading in the environment and/or undergoing chemical treatment.

(e) Candidates for original plastic items

In this section, we discuss the plastic items that could potentially be the origin of the MPs found in Tokyo Bay. First, we focused on the green fragments with rounded shape, as shown in Fig. S1(c), because 19% of the particles of the fragment type were green (Fig. 4a-i). The polymer type of green fragments was mainly PE. Similar green fragments of PE have been found on beaches around Sagami Bay, Japan (e.g., Ikegai et al., 2018), the source of which was identified as artificial grass because artificial grass for home use is made of PE. Hence, artificial grass

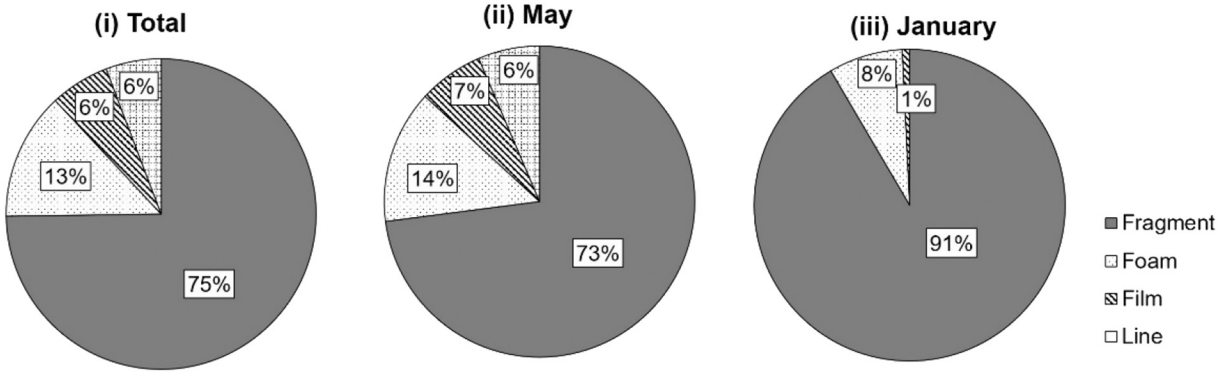

Fig. 3. Percentage of shape type: (a) Total, (b) May, and (c) January.

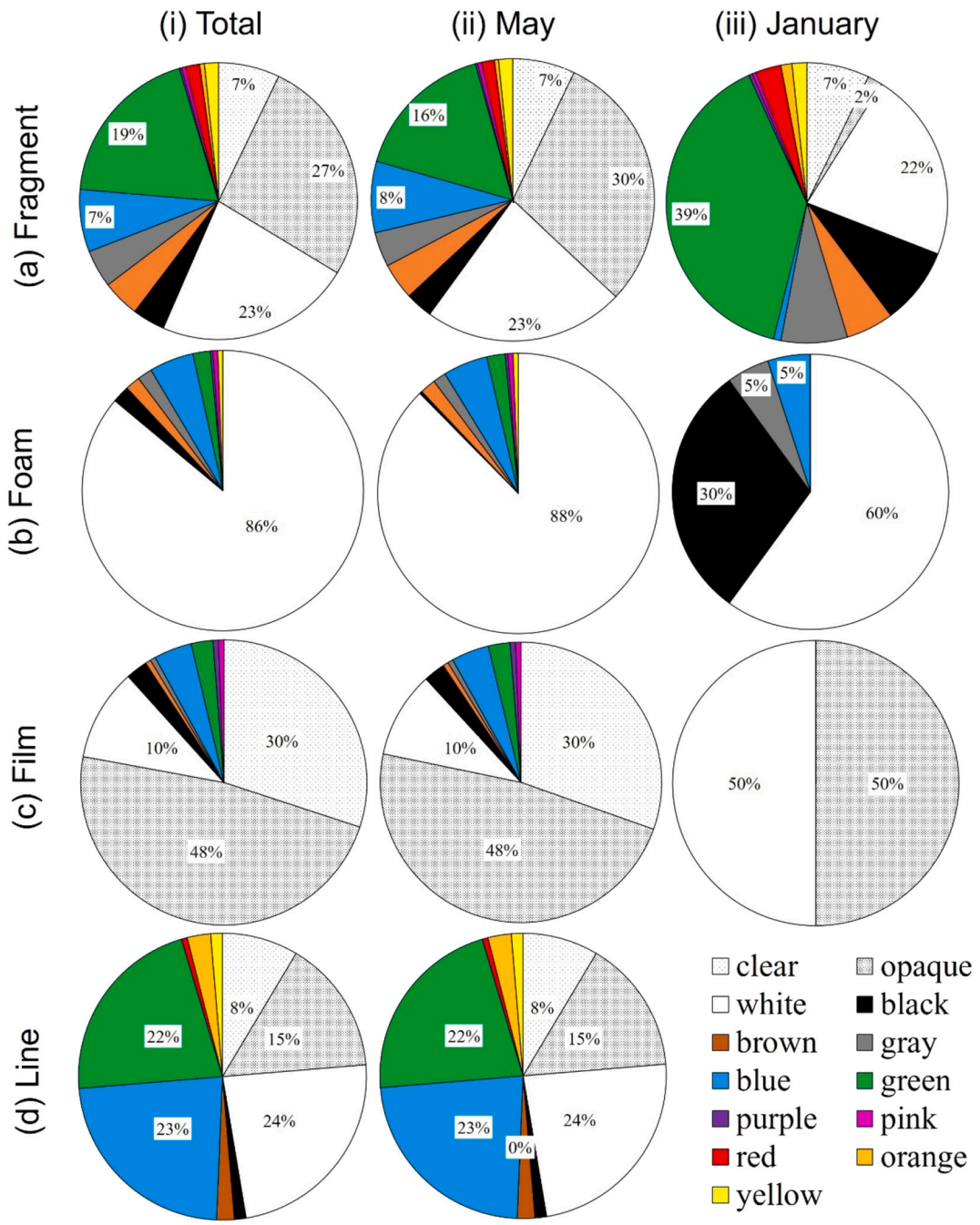

Fig. 4. Percentage of color categorized by shape type: (a) fragment, (b) foam, (c) film, and (d) line (no lines were found in January); (i) Total, (ii) May, and (iii) January.

was considered as one of the origins of the green rounded MPs found in this study.

Next, we focused on original items of line. In Tokyo Bay, as most popular laver culture occurs in winter, line found in May should not be associated with aquaculture. In May, although precipitation is slightly higher, the warm climate encourages fishing as a popular pastime (e.g., Japan Fisheries Agency, 2009); hence, it is conjectured that the difference in the environmental load of line to floating MPs is related to the high levels of recreational fishing activity in May.

3.3. Role of rivers as a source of MPs

We found a difference in the abundance of MPs between May and January (Table 1 and Fig. 2). As previous studies also found that the abundance of MPs on beaches and in rivers in the wet season was markedly greater than in the dry season (e.g., Cheung et al., 2016; Eo et al., 2019), we also compared the abundance of MPs found in the rivers with our results for Tokyo Bay. The mean value of N_{Area} was 0.63 (0.01) pcs/m^2 in May (January) in the inner bay in this study, which is comparable with the estimated abundance of the rivers, i.e., 0.87 (0.07) pcs/m^2 (Fig. 8). This indicates that one of the factors governing the seasonal variation of the abundance of MPs in Tokyo Bay is the seasonal difference in the amount of MPs input via the rivers. However, the abundance of floating MPs in the inner bay was less than that transported via the rivers, which suggests that MPs on the sea surface either sink to the bottom or are transported to outside the bay.

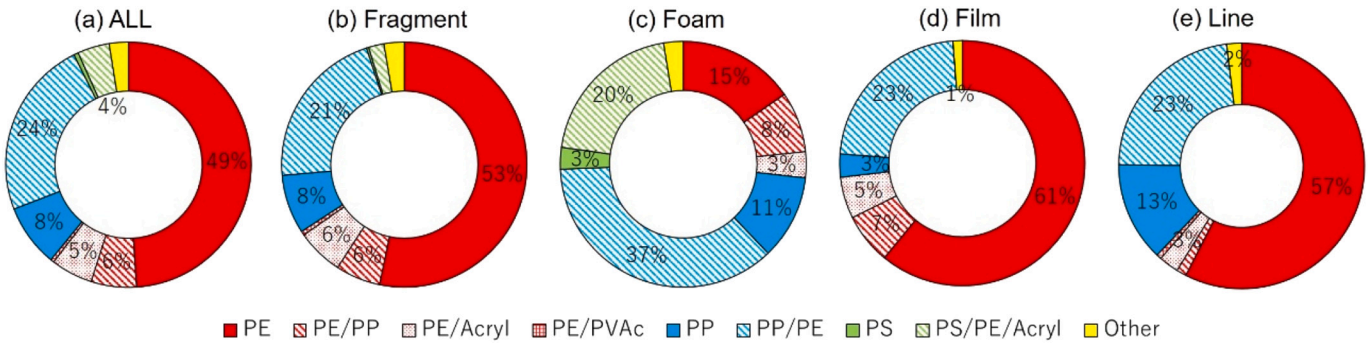

Fig. 5. Percentage of compositions of MPs categorized by shape: (a) secondary MPs, (b) fragment, (c) foam, (d) film, and (e) line. PE/PP and PE/PP indicate co-polymers of PE and PP, where the former composition is the main ingredient of the candidate.

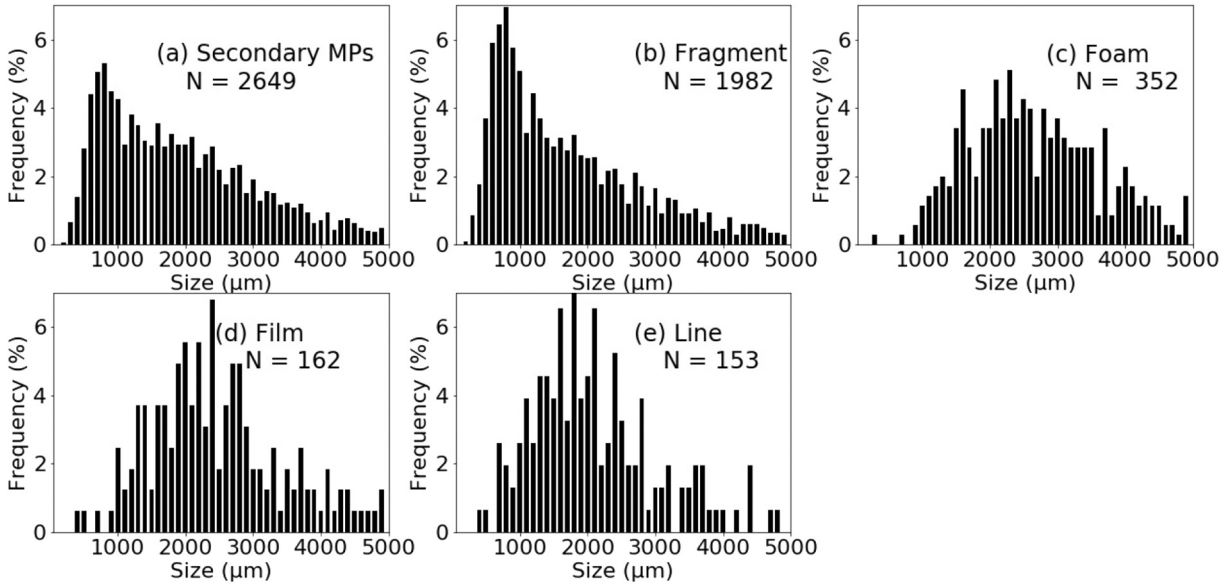

Fig. 6. Size distribution of secondary MPs: (a) total of secondary MPs, (b) fragment, (c) foam, (d) film, and (e) line.

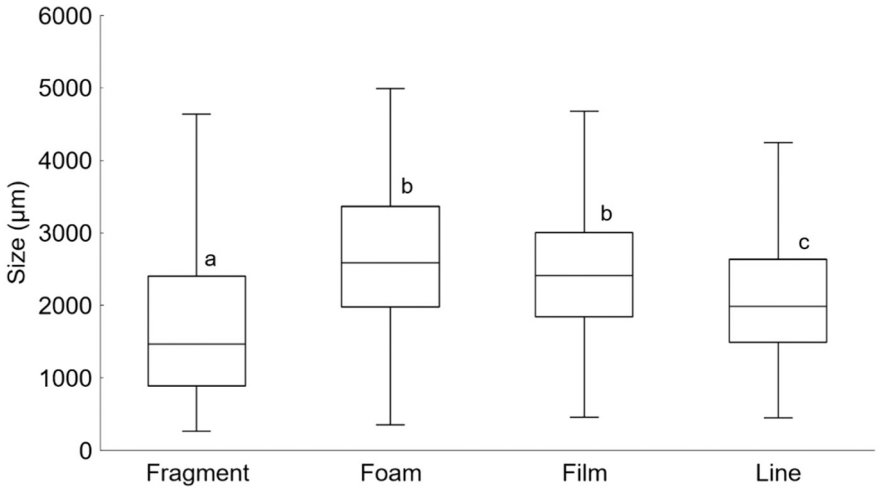

Fig. 7. Box plots of size distribution of secondary MPs. Each shape has different lettering (a–c) to indicate significant difference with $p < 0.01$ using the Steel–Dwass test.

3.4. Destination of MPs in Tokyo Bay

As the density of most pieces of MPs found in the surface waters is lower than that of seawater (PE: 0.91–0.95, PP: 0.90–0.92, and PS: 1.04–1.09; (GESAMP, 2019)), biofilm covering the surface of pieces of MPs is important for increasing their density and causing them to sink.

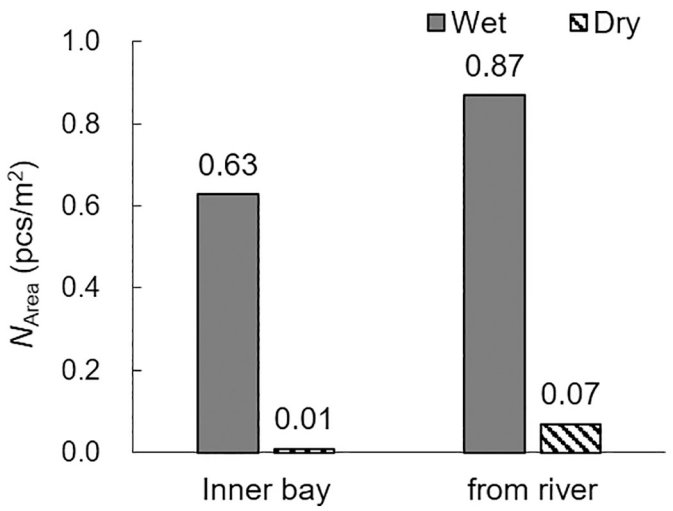

Fig. 8. Abundance of MPs per area in inner bay (observational results and estimates via rivers). Wet represents May data; Dry represents January (December) data for observations (estimates).

Karlsson et al. (2018) found that the weight of plastic film was increased owing to biofilm coverage; however, the apparent density (1000 kg/m^3) was insufficient to cause the plastic to sink. The biofilm in their study developed over a 12-week period on plastic film dipped in ocean water. Thus, if floating MPs were to sink to the bottom because of the development of biofilm, the MPs would be required to remain in Tokyo Bay for at least 12 weeks; however, the annual mean residence time of most river water in the inner bay is 7 weeks (Okada et al., 2007). As this residence time is shorter than the time required for the apparent density to become >1020 kg/m^3, most floating MPs detected by neuston nets would be transported outside of Tokyo Bay. However, Matsuguma et al. (2017) found that small MPs with size of <1000 μm accounted for the majority of MPs found in the sediment of Tokyo Bay. This means that we should consider the fate of MPs categorized by size. Based on the findings of this study, we concluded that Tokyo Bay functions as a source of supply of large MPs (>1000 μm) to the open ocean.

As concentrations of hazardous chemicals found in large particles of MPs were comparable to those in small particles (Tokyo Bay; Yeo et al., 2019), large particles of MPs could export significant portions of Persistent Organic Pollutants (POPs) and additives to the open ocean. Therefore, rapid transportation of large particles of MPs to outside of Tokyo Bay should lead to unexpected transportation of hazardous chemicals to regions outside of the bay.

3.5. Seasonal variation in distribution pattern of MPs

Although the major reason for the seasonal difference in the abundance of MPs was the fact that MPs are transported via rivers, we found local spots with large abundance of MPs to the north of Kannonzaki in May (Stn. S03) and near the mouth of the bay in January (Stn. S08, Fig. 2). As the marine environment of Tokyo Bay depends largely on the circulation pattern that is controlled by river inflows and wind systems (e.g., Sato, 1989; Suzuki et al., 2012), the distribution pattern of MPs should be affected by the physical oceanographic conditions of the bay. Therefore, we examined the relationship between MPs distribution and the oceanographic conditions of the bay.

First, we focused on the pattern of surface currents in Tokyo Bay because Zheng et al. (2019) highlighted that the residual currents are correlated with the distribution of MPs. Suzuki et al. (2012) investigated the monthly residual currents in Tokyo Bay and found definite seasonal variation (arrows in Fig. 2). During April–May, the residual current gradually constructs a clockwise circulation in the northern part of Tokyo Bay (north side of Haneda), with current vectors directed toward the western coast in southern parts (between Haneda and Kannonzaki). During January–March, although the pattern of the residual currents is almost the same as in May, the currents are weaker. Considering the residual currents, MPs should be transported toward Stn. S03. Furthermore, given the seasonality of the abundance of MPs discussed in Section 3.3, we found that Stn. S03 had high abundance of MPs in May.

Next, we considered the existence of a strong front in the bay mouth between Kannonzaki and Futtsu (dashed lines in Fig. 2; Yanagi et al., 1989). This front develops gradually in early winter (November) and then slowly disappears in late winter (March). Generally, the front acts as convergence area in which floating debris accumulates (e.g., Miyao and Isobe, 2016). The location of Stn. S08 is just to the south of this front; thus, the slightly elevated abundance of MPs in January was due to the convergence process at this front.

4. Conclusions

This study focused on MPs suspended in the surface waters of Tokyo Bay. The abundance of MPs was comparable with that of other highly polluted areas; however, the abundance of MPs in Tokyo Bay was less than found in other semi-closed bays because of its geographic characteristics. Fragments of PE accounted for most of the MPs found in Tokyo Bay; however, many copolymers were also found. As small particles are likely to become decolorized more easily than large ones, the larger particles were most suitable for identifying the plastic items that could potentially be the origin of the MPs. From the detailed information derived regarding the MPs, we concluded that artificial grass and fishing gear were one of the sources of green fragments and line, respectively. We found the same seasonality in the abundance of MPs in the bay and as in the rivers. It was concluded that MPs are transported to outside of the bay because of the lower abundance of MPs in the inner bay and the short residence time of the water. The distribution of MPs was found strongly correlated with the residual currents and the seasonal thermohaline front. Based on the above, we conclude that geographic characteristics, abundance of MPs from rivers, and physical oceanographic conditions have a substantial impact on MPs pollution in a semi-closed bay.

Funding

This study was supported by the Environmental Research and Technology Development Fund (JPMEERF18S20208) of the Ministry of the Environment, Japan.

CRediT authorship contribution statement

Haruka Nakano: Ideas; Formal analysis; Investigation; Roles/Writing - original draft.

Hisayuki Arakawa: Resources; Writing - review & editing; Project administration; Supervision; Funding acquisition.

Tadashi Tokai: Writing - review & editing; Project administration; Funding acquisition.

Declaration of competing interest

The authors declare that they have no known competing financial interests or personal relationships that could have appeared to influence the work reported in this paper.

Acknowledgments

We would like to thank Associate Prof. Uchida of Tokyo University of Marine Science and Technology for assistance with the observations. We thank Prof. Yoshida for careful proofreading of the manuscript. We thank Captain Miyazaki and the crews of the T/*V Seiyo-Maru* and R/V *Hiyodori* for supporting the observation campaigns. This study was supported by

the Environmental Research and Technology Development Fund (JPMEERF18S20208) of the Environmental Restoration and Conservation Agency of Japan. We thank Edanz Group (https://en-author-services.edanzgroup.com/) for editing a draft of this manuscript.

Appendix A. Supplementary data

Supplementary data to this article can be found online at https://doi.org/10.1016/j.marpolbul.2020.111887.

References

Andrady, A.L., 2011. Microplastics in the marine environment. Mar. Pollut. Bull. 62 (8), 1596–1605. https://doi.org/10.1016/j.marpolbul.2011.05.030.

Baba Y., and Imamoto H. (1998) A study on the flow in enclosed basins. Annuals of Disas. Prev. Res. Inst., Kyoto Univ., 41, B-2, pp. 333–340.

Bikker, J., Lawson, L., Wilson, S., Rochman, C.M., 2020. Microplastics and other anthropogenic particles in the surface waters of the Chesapeake Bay. Mar. Pollut. Bull. 156, 111257. https://doi.org/10.1016/j.marpolbul.2020.111257.

Chen, M., Jin, M., Tao, P., Wang, Z., Xie, W., Yu, X., Wang, K., 2018. Assessment of microplastics derived from mariculture in Xiangshan Bay, China. Environ. Pollut. 242, 1146–1156. https://doi.org/10.1016/j.envpol.2018.07.133.

Cheung P.K., Cheung L.T.O., and Fok L. (2016) Seasonal variation in the abundance of marine plastic debris in the estuary of a subtropical macroscale drainage basin in South China. Sci. Total Environ., 562. pp. 658–665. https://doi.org/10.1016/j.scitotenv.2016.04.048.

Cohen, J.H., Internicola, A.M., Mason, R.A., Kukulka, T., 2019. Observations and simulations of microplastic debris in a tide, wind, and freshwater-driven estuarine environment: the Delaware Bay. Environ. Sci. Technol. 53, 14204–14211. https://doi.org/10.1021/acs.est.9b04814.

Cózar A., Echevarría F., González-Gordillo J.I., Irigoien X., Úbeda B., Hernández-León S, Palma Á.T., Navarro S., García-de-Lomas J., Ruiz A., Fernández-de-Puelles M.L., Duarte C.M. (2014) Plastic debris in the open ocean. Proc. Natl. Acad. Sci. Jul 2014, 111 (28) 10239–10244; https://doi: https://doi.org/10.1073/pnas.1314705111.

Eo, S., Hong, S.H., Song, Y.K., Han, G.M., Shim, W.J., 2019. Spatiotemporal distribution and annual load of microplastics in the Nakdong River, South Korea. Water Res. 160, 228–2371. https://doi.org/10.1016/j.watres.2019.05.053.

Gago, J., Filgueiras, A., Pedrotti, M.L., Suaria, G., Tirelli, V., Andrade, J., Frias, J., Nash, R., O'Connor, I., Lopes, C., Caetano, M., Raimundo, J., Carretero, O., Viñas, L., Antunes, J., Bessa, F., Sobral, P., Goruppi, A., Aliani, S., Palazzo, L., de Lucia, G.A., Camedda, A., Muniategui, S., Grueiro, G., Fernandez, V., Gerdts, G., 2018. Standardized Protocol for Monitoring Microplastics in Seawater. JPI-Oceans BASEMAN project, p. 34.

GESAMP (2019) Guidelines for the monitoring and assessment of plastic litter and microplastics in the ocean (Kershaw P.J., Turra A. and Galgani F. editors), (IMO/FAO/UNESCO-IOC/UNIDO/WMO/IAEA/UN/UNEP/UNDP/ISA Joint Group of Experts on the Scientific Aspects of Marine Environmental Protection). Rep. Stud. GESAMP No. 99, 130p.

Hanke, G., Werner, S., Galgani, F., Veiga, J.M., and Ferreira, M., (2013) Guidance on monitoring of marine litter in European seas. Joint Research Centre - Scientific and Policy Reports JRC83985 MSFD Technical Subgroup on Marine Litter.

Horton, A.A., Dixon, S.J., 2018. Microplastics: an introduction to environmental transport processes. WIREs Water. 5, e1268 https://doi.org/10.1002/wat2.1268.

Ikegai, T., Mishima, S., Kikuchi, H., Namba, A., Kobayashi, Y., 2018. The characteristics of drifting ashore about microplastics in the coastal area of Sagami Bay. Bulletin of Kanagawa Environmental Research Center 41, 1–10 (In Japanese).

Isobe, A., 2016. Percentage of microbeads in pelagic microplastics within Japanese coastal waters. Mar. Pollut. Bull. 110 (1), 432–437. https://doi.org/10.1016/j.marpolbul.2016.06.030.

Isobe, A., Uchida, K., Tokai, T., Iwasaki, S., 2015. East Asian seas: a hot spot of pelagic microplastics. Mar. Pollut. Bull. 101 (2), 618–623. https://doi.org/10.1016/j.marpolbul.2015.10.042.

Isobe, A., Buenaventura, N.T., Chastain, S., Chavanich, S., Cózar, A., DeLorenzo, M., Hagmann, P., Hinata, H., Kozlovskii, N., Lusher, A.L., Martí, E., Michida, Y., Mu, J., Ohno, M., Potter, G., Ross, P.S., Sagawa, N., Shim, W.J., Song, Y.K., Takada, H., Tokai, T., Torii, T., Uchida, K., Vassillenko, K., Viyakarn, V., Zhang, W., 2019. An interlaboratory comparison exercise for the determination of microplastics in standard sample bottles. Mar. Pollut. Bull. 146, 831–837. https://doi.org/10.1016/j.marpolbul.2019.07.033.

Japan Fisheries Agency (2009) Report on Survey of Recreational Catches in 2009. p1. (In Japanese).

Japan River Association, 2004. River Discharges Yearbook of Japan. Tokyo, Japan (In Japanese).

Karlsson, T.M., Hassellov, M., Jakubowicz, I., 2018. Influence of thermooxidative degradation on the in situ fate of polyethylene in temperate coastal waters. Mar. Pollut. Bull. 135, 187–194. https://doi.org/10.1016/j.marpolbul.2018.07.015.

Kataoka, T., Nihei, Y., Kudou, K., Hinata, H., 2019. Assessment of the sources and inflow processes of microplastics in the river environments of Japan. Environ. Pollut. 244, 958–965. https://doi.org/10.1016/J.ENVPOL.2018.10.111.

Kukulka, T., Proskurowski, G., Moret-Ferguson, S., Meyer, D.W., Law, K.L., 2012. The effect of wind mixing on the vertical distribution of buoyant plastic debris. Geophys. Res. Lett. 39, L07601 https://doi.org/10.1029/2012GL051116.

Masura J., Baker J., Foster G., and Courtney A. (2015) Laboratory methods for the analysis of microplastics in the marine environment: recommendations for quantifying synthetic particles in waters and sediments. NOAA Technical Memorandum NOS-OR&R-48.

Matsuguma, Y., Takada, H., Kumata, H., Kanke, H., Sakurai, S., Suzuki, T., Itho, M., Okazaki, Y., Boonyatumanond, R., Zakaria, M.P., Weerts, S., Newman, B., 2017. Microplastics in sediment cores from Asia and Africa as indicators of temporal trends in plastic pollution. Arch. Environ. Contam. Toxicol. 73, 230–239. https://doi.org/10.1007/s00244-017-0414-9.

Matsumura, T., Ishimaru, T., 2004. Freshwater discharge and inflow loads of nitrogen and phosphorus to Tokyo Bay (from April 1997 to March 1999). Oceanography in Japan 13 (1), 25–36.

McEachern, K., Alegria, H., Kalagher, A.L., Hansen, C., Morrison, S., Hastings, D., 2019. Microplastics in Tampa Bay, Florida: abundance and variability in estuarine waters and sediments. Mar. Pollut. Bull. 148, 97–106. https://doi.org/10.1016/j.marpolbul.2019.07.068.

Michida, Y., Chavanich, S., Chiba, S., Cordova, M.R., Cózar Cabañas, A., Galgani, F., Hagmann, P., Hinata, H., Isobe, A., Kershaw, P., Kozlovskii, N., Li, D., Lusher, A.L., Martí, E., Mason, S.A., Mu, J., Saito, H., Shim, W.J., Syakti, A.D., Agung Dhamar, Takada, H., Thompson, R., Tokai, T., Uchida, K., Vasilenko, K., Wang, J, 2019. Guidelines for Harmonizing Ocean Surface Microplastic Monitoring Methods. Ministry of the Environment Japan 71 pp.

Miyao, Y., Isobe, A., 2016. A combined balloon photography and buoy-tracking experiment for mapping surface currents in coastal waters. J. Atmos. Ocean. Technol. 33, 1237–1250. https://doi.org/10.1175/JTECH-D-15-0113.1.

Munno, K., Helm, P.A., Jackson, D.A., Rochman, C., Sims, A., 2018. Impacts of temperature and selected chemical digestion methods on microplastic particles. Environ. Toxicol. Chem. 37, 91–98. https://doi.org/10.1002/etc.3935.

Nakao, T., Matsuzaki, K., 1995. Potential for eutrophication based on the topography of coastal bays. Oceanography in Japan 4 (1), 19–28.

Okada, T., Takao, T., Nakayama, K., Furukawa, K., 2007. Change in freshwater discharge and residence time of seawater in Tokyo Bay. Japan Society of Civil Engineers. Ser. B 63 (1), 67–72 (In Japanese).

Reisser, J., Slat, B., Noble, K., du Plessis, K., Epp, M., Proietti, M., de Sonneville, J., Becker, T., Pattiaratchi, C., 2015. The vertical distribution of buoyant plastics at sea: an observational study in the North Atlantic gyre. Biogeosciences 12, 1249–1256. https://doi.org/10.5194/bg-12-1249-2015.

Renner, G., Schmidt, T.C., Schram, J., 2018. Analytical methodologies for monitoring micro(nano)plastics: which are fit for purpose? Current Opinion in Environmental Science & Health 1, 55–61. https://doi.org/10.1016/j.coesh.2017.11.001.

Sagawa, N., Kawaai, K., Hinata, H., 2018. Abundance and size of microplastics in a coastal sea: comparison among bottom sediment, beach sediment, and surface water. Mar. Pollut. Bull. 133, 532–542. https://doi.org/10.1016/j.marpolbul.2018.05.036.

Sato, S., 1989. On wind-driven circulation in Tokyo Bay: the case of winter season. Technical Bulletin on Hydrography and Oceanography 8, 1–14 (In Japanese).

Sutton, R., Mason, S.A., Stanek, S.K., Willis-Norton, E., Wren, I.F., Box, C., 2016. Microplastic contamination in the San Francisco Bay, California, USA. Mar. Pollut. Bull. 109, 230–235. https://doi.org/10.1016/j.marpolbul.2016.05.077.

Suzuki K., Isobe M., Yoneyama H., and Nakamura Y. (2012) Effect of the clockwise circulation on the hypoxia at the head of Tokyo Bay. J. Japan Society of Civil Engineers, Ser. B1 (Coastal Engineering), 68(2), I_981–I_985. (In Japanese).

Tanaka K., and Takada H. (2016) Microplastic fragments and microbeads in digestive tracts of planktivorous fish from urban coastal waters. Sci. Rep., 6, 34351. doi.org/10.1038/srep34351.

Yanagi, T., Isobe, A., Saino, T., Ishimaru, T., 1989. Thermohaline front at the mouth of Tokyo Bay in winter. Cont. Shelf Res. 9 (1), 77–91. https://doi.org/10.1016/0278-4343(89)90084-8.

Yeo, B.G., Takada, H., Yamashita, R., Okazaki, Y., Uchida, K., Tokai, T., Tanaka, K., Trenholm, N., 2019. PCBs and PBDEs in microplastic particles and zooplankton in open water in the Pacific Ocean and around the coast of Japan. Mar. Pollut. Bull. 110806 https://doi.org/10.1016/j.marpolbul.2019.110806.

Zaman, A.U., Lehmann, S., 2013. The zero-waste index: a performance measurement tool for waste management systems in a 'zero waste city'. J. Clean. Prod. 50 (1), 123–132.

Zheng Y., Li J., Cao W., Liu X., Jiang F., Ding J., Yin X., Sun C. (2019) Distribution characteristics of microplastics in the seawater and sediment: a case study in Jiaozhou Bay, China. Sci. Total Environ., 674 pp. 27–35. doi:https://doi.org/10.1016/j.scitotenv.2019.04.008.